Aqueous Crystallization of Manganese(II) Group 6 Metal Oxides

Meehae Jang, Timothy J. R. Weakley, and Kenneth M. Doxsee*

Department of Chemistry, University of Oregon, Eugene, Oregon 97403

Received September 19, 2000. Revised Manuscript Received November 23, 2000

Aqueous salt metathesis reactions of manganese(II) salts and various chromate, molybdate, and tungstate salts afford a series of manganese group 6 metal oxides. The chromate reactions form a previously unknown phase, $KMn_2(CrO_4)_2(OH)(H_2O)$ (**1**), whereas the tungstate reactions afford a simpler, hydrated phase, $MnWO_4 \cdot H_2O$ (**4**). In these reactions, the countercation appears to influence the crystal form and size of the products. The molybdate reactions display countercation-dependent phase selectivity. Sodium and ammonium molybdates afford hydrated manganese molybdenum oxide, $MnMoO_4 \cdot H_2O$ (**3**), whereas potassium molybdate affords the new molydenum analogue of the chromate phase, $KMn_2(MoO_4)_2(OH)(H_2O)$ (**2**). Counteranion effects are more subtle, with crystal form and size representing the primary differences between the products from reactions using sulfate, acetate, or chloride salts of manganese(II). Each phase undergoes thermal dehydration, affording α-$MnMoO_4$ from **3** and $MnWO_4$ (hübnerite) from **4**.

Introduction

Manganese molybdenum oxide ($MnMoO_4$) displays interesting magnetic[1] and spectral[2] properties resulting from a complex set of ferromagnetic and antiferromagnetic exchange interactions, and has attracted attention as a catalyst[3,4] for various reactions of hydrocarbons, including the oxidative coupling of methane.[5] Two polymorphs of anhydrous $MnMoO_4$ have been reported. High-temperature solid-state reactions of manganese oxides (MnO, Mn_2O_3, or MnO_2) with MoO_3 afford α-$MnMoO_4$, the polymorph stable under ambient conditions of temperature and pressure,[2,6−8] whereas a second anhydrous phase is obtained from MnO and MoO_3 at 900 °C and elevated pressure.[9] The latter phase has the wolframite structure, typical of a variety of metal tungsten oxides (e.g., $NiWO_4$),[10] with a distorted hexagonal close-packing of oxygen atoms and Mn and Mo atoms each occupying one-fourth of the octahedral interstices. This phase converts to α-$MnMoO_4$ upon heating in air at 600 °C.

Clearfield et al. have reported the preparation of a variety of hydrated manganese(II) molybdenum oxides by aqueous metathesis reactions of manganese(II) sulfate and sodium molybdate.[11] Depending on the pH of the manganese sulfate solution (ranging from 3 to 7.1), three phases of composition $MnMoO_4 \cdot H_2O$ are obtained. Each phase provides a distinctive X-ray powder diffraction pattern, and the structure of the phase obtained from neutral solution was determined by single-crystal X-ray diffraction analysis. Hydrothermal reactions of $MnMoO_4 \cdot H_2O$ with sodium molybdate at 200 °C afford a more complex phase, $NaMn_2(MoO_4)_2(OH)(H_2O)$, structurally characterized by single-crystal X-ray diffraction analysis. This phase is isostructural with sodium zinc molybdate, $NaZn_2(MoO_4)_2(OH)(H_2O)$, prepared hydrothermally from zinc(II) salts and sodium molybdate.[12]

No analogous hydrothermal reaction chemistry appears to have been reported in the chromate series. The solid-state reaction between MnO_2 and CrO_2 produces $CrMnO_4$, formulated as $Cr(III)Mn(V)O_4$ on the basis of crystal data and magnetic properties.[13] Anhydrous manganese(II) tungsten oxide ($MnWO_4$, hübnerite[14]), which has been employed as a component in a humidity sensor,[15,16,17] may be prepared by thermal treatment

(1) Uitert, L. G. V.; Sherwood, R. C.; Williams, H. J.; Rubin, J. J.; Bonner, W. A. *J. Phys. Chem. Solids* **1964**, *25*, 1447. Attfield, J. P. *J. Phys.: Condens. Matter* **1990**, *2*, 6999. Lippold, B.; Herrmann, J.; Reichelt, W.; Oppermann, H. *Phys. Status Solidi* **1991**, *A124*, K59. Lautenschläger, G.; Weitzel, H.; Fuess, H.; Ressouche, E. *Z. Kristallografiya* **1994**, *209*, 936.

(2) Doyle, W. P.; McGuire, G.; Clark, G. M. *J. Inorg. Nucl. Chem.* **1966**, *28*, 1185.

(3) Rajaram, P.; Viswanathan, B.; Sastri, M. V. C.; Srinivasan, V. *Indian J. Chem.* **1974**, *12*, 1267.

(4) Veleva, S.; Trifiro, F. *Kinet. Catal. Lett.* **1976**, *4*, 19.

(5) Driscoll, S.; Ozkan, U. S. *Stud. Surf. Sci. Catal.* **1994**, *82*, 367. Driscoll, S. A.; Zhang, L.; Ozkan, U. S. *Oxidative Coupling of Methane over Alkali-Promoted Simple Molybdate Catalysts: Activation and Selective Oxidation of C_1-C_4 Alkanes*; ACS Symp. Ser. **1993**, No. 523, 340-353. Driscoll, S. *Oxidative Coupling of Methane over Alkali-Promoted $MnMoO_4$ Catalysts*, Ph. D. dissertation, Ohio State University, 1994.

(6) Rajaram, P.; Viswanathan, B.; Aravamudan, G.; Srinivasan, V.; Sastri, M. V. C. *Thermochim. Acta* **1973**, *7*, 123.

(7) Sleight, A. W.; Chamberland, B. L. *Inorg. Chem.* **1968**, *7*, 1672.

(8) Abrahams, S. C.; Reddy, J. M. *J. Chem. Phys.* **1965**, *43*, 2533.

(9) Young, A. P.; Schwartz, C. M. *Science* **1963**, *141*, 348.

(10) Keeling, R. O., Jr. *Acta Crystallogr.* **1957**, *10*, 209.

(11) Clearfield, A.; Moini, A.; Rudolf, P. R. *Inorg. Chem.* **1985**, *24*, 4606.

(12) Clearfield, A.; Sims, M. J.; Gopal, R. *Inorg. Chem.* **1976**, *15*, 335.

(13) Chamberland, B. L.; Kafalas, J. A.; Goodenough, J. B. *Inorg. Chem.* **1977**, *16*, 44.

(14) Gaines, R. V.; Skinner, H. C. W.; Foord, E. E.; Mason, B.; Rosenzweig, A. *Dana's New Mineralogy*, 8th ed.; J. Wiley: New York, 1998; p. 993.

(15) Ichinose, N. *Adv. Sci. Technol. (Faenza, Italy)* **1999**, *26*, 69.

(16) Dellwo, U.; Keller, P.; Meyer, J.-U. *Sens. Actuators B* **1997**, *40* (2−3), 175.

(17) Qu, W.; Meyer, J.-U.; Haeusler, A. *Technisches Messen* **1996**, *63* (3), 105.

10.1021/cm000754c CCC: $20.00 © 2001 American Chemical Society
Published on Web 01/18/2001

(1000 °C, 10 min) of the product of the metathesis reaction between manganese(II) chloride and sodium tungstate.[18] Hübnerite adopts at least three antiferromagnetic phases in zero field and as a result displays unusual magnetic properties; e.g., the low-temperature phase exhibits a magnetic unit cell 16 times larger than the crystallographic unit cell.[19]

We report here the synthesis of hydrated manganese group 6 metal oxides by aqueous salt metathesis reactions under ambient conditions of temperature and pressure. As discussed below, we have observed an interesting cation-dependent phase selectivity in the molybdate series, with sodium and ammonium molybdate affording $MnMoO_4 \cdot H_2O$, but potassium molybdate affording the previously unknown complex oxide $KMn_2(MoO_4)_2(OH)(H_2O)$. In addition, we have prepared a series of new chromate phases of analogous structure, $YMn_2(CrO_4)_2(OH)(H_2O)$ (Y = Na, K, NH_4), and have observed cation-dependent alteration of the crystal habit of hydrated $MnWO_4$.

Experimental Section

Materials. Manganese(II) sulfate monohydrate (Mallinckrodt), $MnCl_2$ (Alfa), 1,4,7,10,13,16-hexaoxacyclooctadecane (18-crown-6, Janssen), and K_2CrO_4 (Baker) were used as obtained from the indicated sources. Manganese(II) acetate, $(NH_4)_2CrO_4$, K_2MoO_4, $Na_2MoO_4 \cdot 2H_2O$, $(NH_4)_2MoO_4$, K_2WO_4, $Na_2WO_4 \cdot 2H_2O$, $(NH_4)_2WO_4$, tris[2-(2-methoxyethoxy)ethyl]amine (MEEA), poly(vinyl alcohol) (MW 13,000−23,000, 87% hydrolyzed), and methanol were used as received from Aldrich Chemical Co.

Instrumentation. X-ray powder diffraction analyses were performed on a Scintag powder diffractometer using Cu Kα radiation. SEM images were obtained on a JEOL JSM-6300XV digital scanning electron microscope equipped with an Oxford/Link eXL energy-dispersive X-ray (EDX) detector. Thermogravimetric analysis was performed on a TGA model 951 and differential scanning calorimetry on a DuPont Instruments model 510 instrument. Single-crystal structural analysis of $KMn_2(MoO_4)_2(OH)(H_2O)$ (**2**) was carried out on an Enraf-Nonius CAD-4 diffractometer.

Preparation of $KMn_2(CrO_4)_2(OH)(H_2O)$ (1). A test tube (2 cm diameter, 30 mL volume) was charged with 7 mL of a 0.05 M aqueous solution of K_2CrO_4 in water. A glass microfiber filter paper (Whatman, 2.5 cm diameter) was placed in contact with the surface of the solution. Pure water (5 mL) was added, followed by a second filter paper. On this was layered 5 mL of a 0.05 M aqueous solution of $MnSO_4 \cdot H_2O$. The tube was capped with a rubber septum and allowed to stand under ambient laboratory conditions (ca. 22 °C) for several days. A dark-brown powder precipitated onto the filter papers, and the walls of the tube took on the same dark-brown color. The product clings tenaciously to both the walls of the tube and the filter papers, but a low yield (<5%) of solid was isolated by careful scraping of the papers. Both X-ray powder diffraction analysis and scanning electron microscopy suggest that the bulk of the product remains tightly associated with the filter papers.

Slow crystallization, by either using less concentrated solutions of the reactants (<0.02 M) or diffusion of the reactant solutions into a poly(vinyl alcohol) gel, resulted in uniform coating of all glass surfaces and filter paper fibers with a thin dark-brown film. Rapid precipitation from >0.07 M solutions of reactants, omitting the glass fiber filter papers, afforded the product as a dark-brown powder in >70% yield.

Table 1. Crystallographic Data for $KMn_2(MoO_4)_2(OH)(H_2O)$ (1)

composition	$H_3KMn_2Mo_2O_{10}$
formula wt	503.87
space group	*C*2/*m*
a	9.7233(13) Å
b	6.6838(10) Å
c	7.8774(10) Å
β	116.220(11)°
V	459.3(1) Å^3
Z	2
d_{calc}	3.643 g-cm^{-3}
T	22 °C
λ	0.71073 Å
μ	58.4 cm^{-1}
rel. trans. coeff.	0.96−1.00 (Ψ)
no. obs. reflns.	651 [I≥ 1.5*σ*(I)]
R(*F*), *wR*(*F*)[a]	0.025, 0.034

[a] $R(F) = \Sigma||F_o| - |F_c||/\Sigma|F_o|$; $wR(F) = [\Sigma_w(|F_o| - |F_c|)^2/\Sigma_w|F_o|^2]^{1/2}$.

Preparation of $KMn_2(MoO_4)_2(OH)(H_2O)$ (2). A test tube (2 cm diameter, 30 mL volume) was charged with 5 mL of a 0.05 M aqueous solution of $MnSO_4 \cdot H_2O$. A glass microfiber filter paper (Whatman, 2.5 cm diameter) was placed in contact with the surface of the solution. Pure water (3 mL) was added, followed by a second filter paper. On this was layered 5 mL of a 0.05 M aqueous solution of K_2MoO_4. The tube was capped with a rubber septum and allowed to stand under ambient laboratory conditions (ca. 22 °C) for 4 days. The light-yellow powder that formed on the bottom of the test tube was isolated by filtration, washed with water and acetone, and dried (89%).

The preparation was also carried out in a U-tube configuration. Water (12 mL) was placed in a U-tube (1.8 cm diameter, 40 mL volume), and glass fiber filter papers were inserted to cover each solvent surface. To the sidearms were then carefully added 0.02 M aqueous solutions of $MnSO_4 \cdot H_2O$ and K_2MoO_4. After 1 month at ca. 22 °C, glistening yellow crystals were evident throughout the tube. The product, isolated as described above, was suitable for single-crystal X-ray diffraction analysis (vide infra).

Preparation of $MnMoO_4 \cdot H_2O$ (3). Replacement of K_2MoO_4 with $Na_2MoO_4 \cdot 2H_2O$ or $(NH_4)_2MoO_4 \cdot 2H_2O$ in the above procedure afforded $MnMoO_4 \cdot H_2O$ as a pink-tinged tan solid (84%) (after 7 days; see Discussion).

Preparation of $MnWO_4 \cdot H_2O$ (4). Replacement of K_2MoO_4 with K_2WO_4, $Na_2WO_4 \cdot 2H_2O$, or $(NH_4)_2WO_4$ in the above procedure afforded $MnWO_4 \cdot H_2O$ as a yellowish powder (98%).

X-ray Diffraction Analysis of $KMn_2(MoO_4)_2(OH)(H_2O)$ (2). A pale-yellow crystal of dimensions 0.05 × 0.07 × 0.11 mm was mounted on a fiber. The orientation parameters and cell dimensions were obtained from the diffractometer setting angles for 25 centered reflections in the range $13.3° \leq \theta \leq 14.5°$. The absence of general reflections *hkl* with $(h + k)$ odd in this range, together with *b* and $a + b$ axial photographs, confirmed that the cell was C-centered monoclinic. Table 1 contains a summary of crystal data and the final residuals. A more extensive table including particulars of data collection and structure refinement is included in the Supporting Information. Absorption corrections appeared unnecessary. All non-hydrogen atoms were located by direct methods (SIR92).[20] Hydrogen atoms were located in difference syntheses and included in the calculations without refinement [H(2) as a half-atom]. The final difference synthesis was featureless. The teXsan program suite[21] was used in all calculations. The K, Mn, and Mo atoms lie at special positions of symmetry 2/*m*, *I*, and *m*, with octahedral, octahedral, and tetrahedral coordination geometry, respectively. The H(2) atoms, bonded to O(4), half-occupy sites close to a center of symmetry so that the structure is a superposition of H(1)−O(4)−H(2)···O(4)−H(1)

(18) Swanson, H. E.; Morris, M. C.; Stinchfield, R. P.; Evans, E. H. *Natl. Bur. Stds. Monogr.* **1963**, *25*, 24.

(19) Ehrenberg, H.; Weitzel, H.; Fuess, H. *Phys. Rev. B: Condens. Matter* **1997**, *234*−*236*, 560. Ehrenberg, E.; Weitzel, H.; Heid, C.; Fuess, H.; Wltschek, G.; Kroener, T.; van Tol, J.; Bonnet, M. *J. Phys.: Condens. Matter* **1997**, *9*, 3189.

(20) Altomare, A.; Cascarano, G.; Giacovazzo, C.; Guagliardi, A.; Burla, M. C.; Polidori, G.; Camalli, N. *J. Appl. Crystallogr.* **1994**, *27*, 435.

(21) *TeXsan Software for Single-Crystal Structure Analysis*, ver. 1.7; Molecular Structures Corporation: The Woodlands, TX, 1997.

Table 2. Atomic Coordinates and Equivalent Isotropic Thermal Parameters [$B_{eq} = 8\pi^2/3)\Sigma_i\Sigma_j U_{ij} a^*_i a^*_j a_i \cdot a_j$] (Å^2) for $KMn_2(MoO_4)_2(OH)(H_2O)$ (1)

atom	x	y	z	B_{eq}
Mo	0.08427(5)	0.0000	0.28706(6)	0.782(9)
Mn	0.2500	0.2500	0.0000	1.27(2)
K	0.0000	0.5000	0.5000	1.42(3)
O1	0.2177(5)	0.0000	0.5221(6)	1.80(9)
O2	−0.0321(3)	0.2142(5)	0.2397(4)	1.31(5)
O3	0.1870(5)	0.0000	0.1439(6)	1.33(8)
O4	0.3500(5)	0.0000	−0.0861(6)	1.19(8)
H1	0.327	0.000	−0.206	1.5
H2	0.438	0.000	−0.052	1.5

Table 3. Bond Lengths (Å) for $KMn_2(MoO_4)_2(OH)(H_2O)$ (1)

bond	length
Mo−O1	1.729(4)
Mo−O2	1.760(3)
Mo−O3	1.807(4)
Mn−O2	2.140(3)
Mn−O3	2.251(3)
Mn−O4	2.186(3)
K−O1[a]	2.826(5)
K−O2	2.717(3)

[a] $-1/2 + x$, $1/2 + y$, z.

Table 4. Bond Angles (°) for $KMn_2(MoO_4)_2(OH)(H_2O)$ (1)

bond	angle	bond	angle
O1−Mo−O2	109.6(1)	O1−K−O2′	75.19(9)
O1−Mo−O3	108.0(2)	O2−K−O2′	90.7(1)
O2−Mo−O2′	108.9(2)	O2−K−O2″	180.00
O2−Mo−O3	110.4(1)	O2′-K−O2″	89.3(1)
O2−Mn−O2′	180.00	Mo−O1−K	102.9(3)
O2−Mn−O3	88.7(1)	Mo−O2−Mn	124.8(2)
O2−Mn−O4	92.5(1)	Mo−O2−K	124.3(1)
O3−Mn−O3′	180.00	Mn−O2−K	109.0(1)
O3−Mn−O4	81.1(1)	Mo−O3−Mn	131.51(8)
O4−Mn−O4′	180.00	Mn−O3−Mn	95.9(2)
O1−K−O1′	180.00	Mn−O4−Mn	99.7(2)
O1−K−O2	104.81(9)		

and H(1)−O(4)···H(2)−O(4)−H(1). Final atomic coordinates and thermal parameters are presented in Table 2, and Tables 3 and 4 report relevant bond lengths and angles, respectively.

Results and Discussion

Chromates. The aqueous salt metathesis reaction between $MnSO_4 \cdot H_2O$ and K_2CrO_4 affords a dark-brown crystalline solid. Using reactant solution concentrations of 0.05 M or higher in simple liquid−liquid interdiffusion experiments, with the reacting solutions separated by glass fiber filter papers, crystallization is quite rapid. However, only very small amounts of the product are recoverable from the filter papers on which it is deposited. Interestingly, both the filter papers and the test tube become coated with a thin brown layer of the product, which clings tenaciously to glass surfaces. Scanning electron microscopy of the product, both as deposited on the filter papers (Figure 1) and as isolated as a free-flowing powder (Figure 2), demonstrates a high degree of crystallinity, but also reveals the proclivity of the product to undergo extensive twinning. To reduce twinning, crystallization from solutions of lower concentration (<0.02 M) was attempted. Unfortunately, under these conditions, the entire product is deposited as an essentially unrecoverable polycrystalline film on the filter papers and on the glass test tube surfaces, all of which become dark-brown. Similarly, crystallization within an aqueous poly(vinyl alcohol) gel (4 wt %) results only in coating of the walls of the test tube. Rapid precipitation from more concentrated solutions (>0.07 M) affords the product as a free-flowing powder in higher isolable yield (>70%), but the so-formed product is comprised of appreciably smaller crystals, as judged by both X-ray powder diffraction pattern peak widths and scanning electron microscopy. Attempts to alter the crystallization behavior of this material by the addition of chelating agents[22] (tris[2-(2-methoxyethoxy)-ethyl]amine in the $MnSO_4 \cdot H_2O$ solution or 18-crown-6 in the K_2CrO_4 solution) were unsuccessful, affording essentially amorphous material.

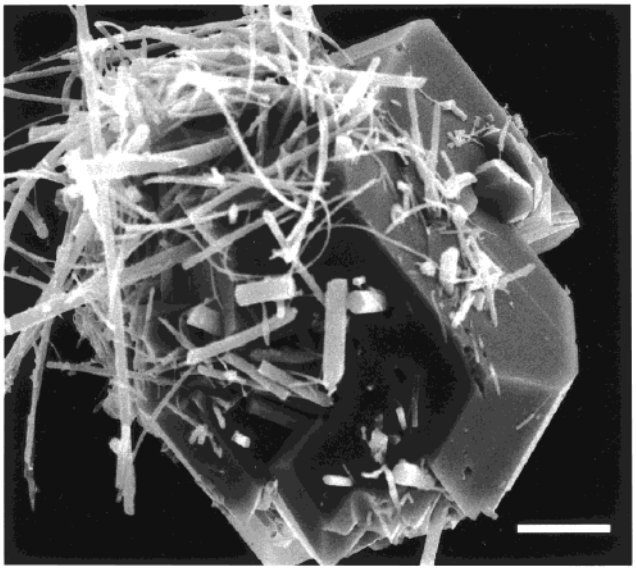

Figure 1. Scanning electron microscopic image of $KMn_2(CrO_4)_2(OH)(H_2O)$, showing intimate association with glass fibers of filter paper. Bar = 10 μm.

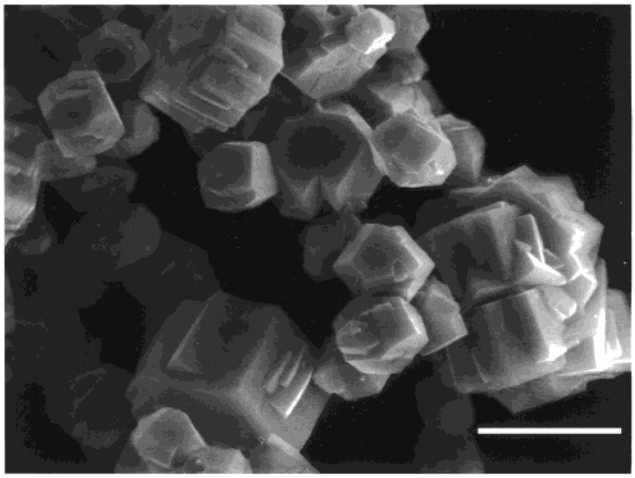

Figure 2. Scanning electron microscopic image of complexly twinned crystals of $KMn_2(CrO_4)_2(OH)(H_2O)$. Bar = 10 μm.

EDX analysis of the product reveals the presence of manganese, chromium, and potassium. The extensive twinning displayed by the product has thus far precluded successful structure determination by single-crystal X-ray diffraction analysis. However, X-ray powder diffraction analysis (Figure 3, Table 5) clearly displays the product to be essentially isomorphous with

(22) For example, see: Doxsee, K. M.; Jang, M. *Mater. Res. Soc. Symp. Proc.* **1998**, *495*, 209.

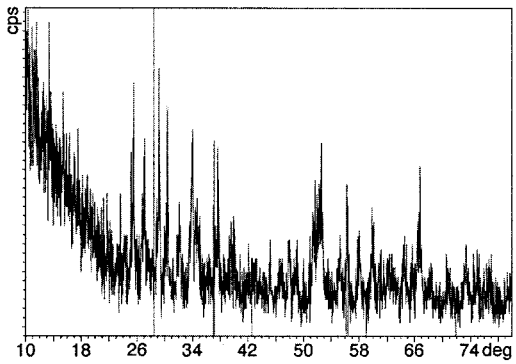

Figure 3. X-ray powder diffraction pattern of $KMn_2(CrO_4)_2(OH)(H_2O)$.

Table 5. X-ray Powder Patterns of $KMn_2(MO_4)_2(OH)(H_2O)$ (M = Mo, Cr)

$KMn_2(MoO_4)_2(OH)(H_2O)$		$KMn_2(CrO_4)_2(OH)(H_2O)$	
d, Å	I/I_o, %	*d*, Å	I/I_o, %
5.189	58	3.479	93
4.842	26	3.293	61
3.733	17	3.053	100
3.612	46	2.929	83
3.352	100	2.781	40
3.304	42	2.632	73
3.149	22	2.409	27
3.105	40	2.381	64
2.987	31	2.256	33
2.891	47	2.002	22
2.715	73	1.894	23
2.651	17	1.778	38
2.629	24	1.738	71
2.611	26	1.660	30
2.404	14	1.633	57
2.274	27	1.588	32
1.953	19	1.544	41
1.925	24	1.459	20
1.824	35	1.398	61
1.793	30		
1.758	15		
1.686	21		
1.661	53		
1.466	29		

the molybdate analogue (vide infra), and thus we formulate it as the previously unknown phase, $KMn_2(CrO_4)_2(OH)(H_2O)$ (**1**). Thermogravimetric analysis (TGA) of the product, quantitatively similar to that of the molybdenum analogue, confirms the presence of water (Table 6). In contrast to the results in the molybdenum series (vide infra), the same manganese chromium oxide phase is obtained when Na_2CrO_4 or $(NH_4)_2CrO_4$ is used in place of K_2CrO_4 as the source of chromate.

Molybdates. Salt metathesis reactions between $MnSO_4 \cdot H_2O$ and K_2MoO_4 in aqueous solution in simple liquid−liquid interdiffusion experiments, with the reacting solutions separated by glass fiber filter papers, afford a coarsely crystalline light-yellow product in good yield (89%). In contrast to the chromate reaction, in which crystallization appears to occur preferentially on glass surfaces, the molybdenum compound is easily isolated as a crystalline solid. The X-ray powder diffraction pattern of this solid (Figure 4, Table 5), notably similar to that of the chromium analogue, does not match the reported pattern for either α-$MnMoO_4$ or any of the three known phases of $MnMoO_4 \cdot H_2O$. Scanning electron microscopy shows the compound to be well crystallized (Figure 5), and EDX analysis reveals the presence of potassium in addition to the anticipated manganese and molybdenum. Interestingly, the crystal form of this material is markedly dependent on the nature of the manganese precursor, with $MnSO_4 \cdot H_2O$ affording the prismatic forms illustrated in Figure 5, but $MnCl_2$ giving rise to more heavily faceted and less elongated forms.

Crystals of the product suitable for single-crystal X-ray diffraction analysis were grown from 0.02 M solutions of $MnSO_4 \cdot H_2O$ and K_2MoO_4 in a U-tube apparatus, with pure water separating the reactant solutions contained in the sidearms of the tube. The X-ray structural analysis displays the product to be $KMn_2(MoO_4)_2(OH)(H_2O)$ (**2**) (Figure 6). Compound **2** is isostructural with the sodium analogue, $NaMn_2(MoO_4)_2(OH)(H_2O)$, reported by Clearfield et al.[11] Interestingly, whereas the sodium analogue apparently required hydrothermal synthesis at 200 °C, the potassium compound is reproducibly accessed from aqueous solution under ambient conditions of temperature and pressure. As noted earlier for both the sodium and the zinc analogues, the positions of the hydrate and the hydroxide moieties are disordered.[11,12] Isolated MoO_4 tetrahedra form parallel chains along the (010) direction, generating channels in which are contained the potassium ions. Molybdenum−oxygen bond lengths in the MoO_4 tetrahedra range from 1.729(4) to 1.807(4) Å, averaging 1.765 Å; both the average length and the spread in values are very similar to those reported for $NaZn_2(MoO_4)_2(OH)(H_2O)$ and for α-$MnMoO_4$ and are as expected for tetrahedral coordination.[23−25] The O−Mo−O bond angles, averaging 109.2°, display an appreciably smaller range (2.4°) than those in α-$MnMoO_4$ (4.5° and 11.5° for two crystallographically independent MoO_4 units).[8]

The potassium ions are octahedrally coordinated by six oxygen atoms from MoO_4 units. The average potassium−oxygen bond length, at 2.772 Å, is within the expected range, and the O−K−O bond angles average 90.0°, although the individual O−K−O angles span a rather wide range, from 75.19° to 104.81°. The Mn(II) cation is pseudo-octahedrally coordinated to oxygen atoms of the MoO_4 tetrahedra (O2 and O3) and of the H_2O and OH^- moieties. The manganese−oxygen bond lengths average 2.192 Å, somewhat longer than that seen in α-$MnMoO_4$ (ca. 2.164 Å),[8] but still within typical bonding range and perhaps consistent with the more open structure imposed on **2** by hydration and the presence of potassium ions. With two short, two intermediate, and two longer Mn−O bonds, the octahedral coordination about manganese is similar to that seen for one of the two independent manganese atoms in α-$MnMoO_4$, although the spread in values for **2** (0.111 Å) is narrower than that for α-$MnMoO_4$ (0.136 and 0.154 Å for the two independent manganese atoms). Oxygen−manganese−oxygen bond angles average 87.4°, similar to those in α-$MnMoO_4$ and consistent with pseudo-octahedral coordination.

As for the chromium analogue (**1**), thermogravimetric analysis of **2** reveals loss of water upon heating (Table

(23) Abrahams, S. C. *J. Chem. Phys.* **1967**, *46*, 2052.
(24) Abrahams, S. C.; Bernstein, J. L.; Jamieson, P. B. *J. Chem. Phys.* **1968**, *48*, 2619.
(25) Kihlborg, L.; Norrestam, R.; Olivecrona, B. *Acta Crystallogr., Sect. B* **1971**, *27*, 2066.

Table 6. Thermogravimetric Analysis[a]

compound	cmpd no.	% wt loss (exptl)	% wt loss (calcd for 1 H_2O)	% wt loss (calcd per eq 1)
$KMn_2(CrO_4)_2(OH)(H_2O)$	**1**	5.5	4.3	6.5
$KMn_2(MoO_4)_2(OH)(H_2O)$	**2**	5.2	3.6	5.4
$MnMoO_4 \cdot H_2O$	**3**	7.3	7.7	na[b]
$MnWO_4 \cdot H_2O$	**4**	3.8	5.6	na[b]

[a] Samples contained in aluminum pans and using a heating rate of 10 °C min^{-1}, with a dry N_2 purge of 40 mL min^{-1}. [b] na = not applicable.

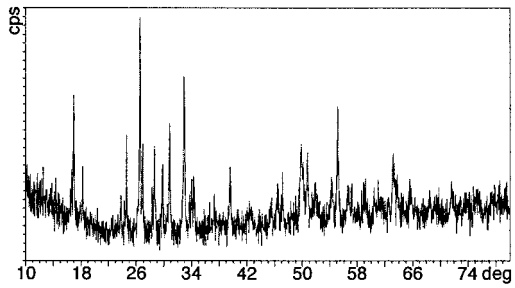

Figure 4. X-ray powder diffraction pattern of $KMn_2(MoO_4)_2(OH)(H_2O)$.

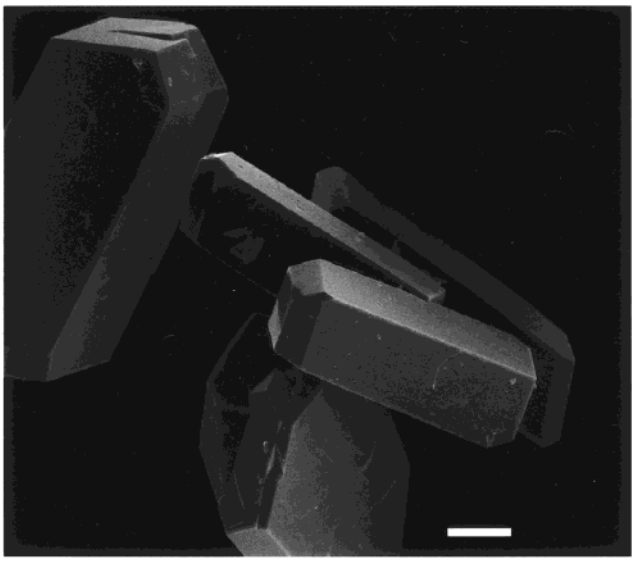

Figure 5. Scanning electron microscopic image of $KMn_2(MoO_4)_2(OH)(H_2O)$. Bar = 20 μm.

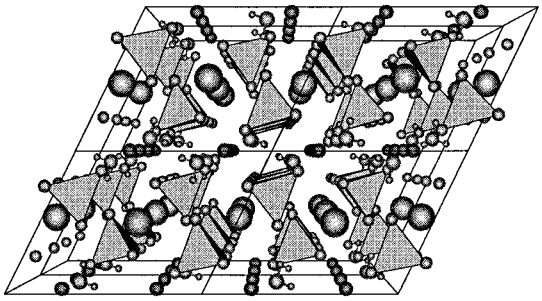

Figure 6. Structure of $KMn_2(MoO_4)_2(OH)(H_2O)$ as determined by single-crystal X-ray diffraction analysis: tetrahedra = MoO_4 units, large spheres = K, small dark spheres = Mn, small light spheres = O, and smallest spheres = H.

6). The observed weight loss for both the chromium (5.5%) and molybdenum (5.2%) compounds is greater than expected for a simple monohydrate, and is consistent with loss of hydroxide as well as water, according to eq 1 (M = Cr, Mo) [calculated loss 6.5% (Cr), 5.4% (Mo)]. Mass loss occurs in two stages under an N_2 atmosphere, the first commencing at ca. 245 °C and the second at ca. 302 °C. Although quantitative determination of the weight loss in each stage is hindered by the overlap of the two thermal events, ca. 3% weight loss appears to occur during the lower temperature event, consistent with loss of the first two waters (as per eq 1) at this time. X-ray powder diffraction analysis after the TGA study confirms the disappearance of **2** (Figure 7), but the nature of the resulting crystalline phase(s) has not been established.

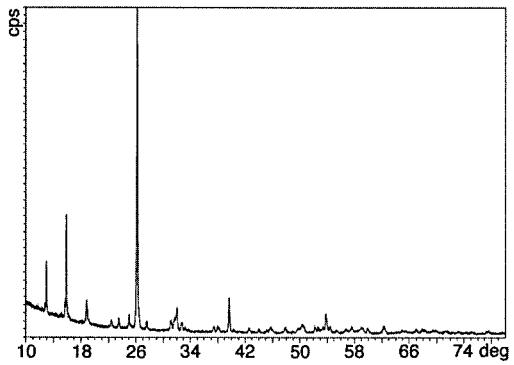

Figure 7. X-ray powder diffraction pattern of $KMn_2(MoO_4)_2(OH)(H_2O)$ following thermal dehydration.

$$2KMn_2(MO_4)_2(OH)(H_2O) \rightarrow 3H_2O + [KMn_2(MO_4)_2]_2 \cdot O \quad (1)$$

Under identical conditions, the metathesis reaction between $MnSO_4 \cdot H_2O$ and the sodium salt, Na_2MoO_4, does not afford the sodium analogue of (**2**), but rather a hydrated manganese molybdate phase, $MnMoO_4 \cdot H_2O$ (**3**). This phase appears identical to that reported by Clearfield et al. for the metathesis reaction in neutral aqueous solution. Under our conditions, $MnMoO_4 \cdot H_2O$ is obtained as a pink-tan crystalline solid. Scanning electron microscopy reveals the presence of highly twinned aggregates (Figure 8A), and EDX analysis of multiple samples consistently reveals the presence of only manganese and molybdenum, with no evidence for alkali metal incorporation. Thermogravimetric analysis (Table 6) reveals a dehydration event commencing at ca. 200 °C and completed by 370 °C (weight loss 7.3%, vs 7.7% calculated for the monohydrate). Following this thermal analysis, X-ray powder diffraction analysis confirms the formation of anhydrous α-$MnMoO_4$.[8]

Interestingly, no precipitation is observed upon initial mixing of aqueous solutions of Na_2MoO_4 and $MnSO_4 \cdot H_2O$. Over a several hour period, slender, pale-yellow needles separate from the reaction mixture. Isolation at this point affords a compound displaying an X-ray powder diffraction pattern resembling that of **2**, suggesting it to be the sodium analogue, $NaMn_2(MoO_4)_2(OH)(H_2O)$. If the reaction mixture is allowed to stand for several days before product isolation, the pale-yellow needles are replaced by the pink-tinged crystalline

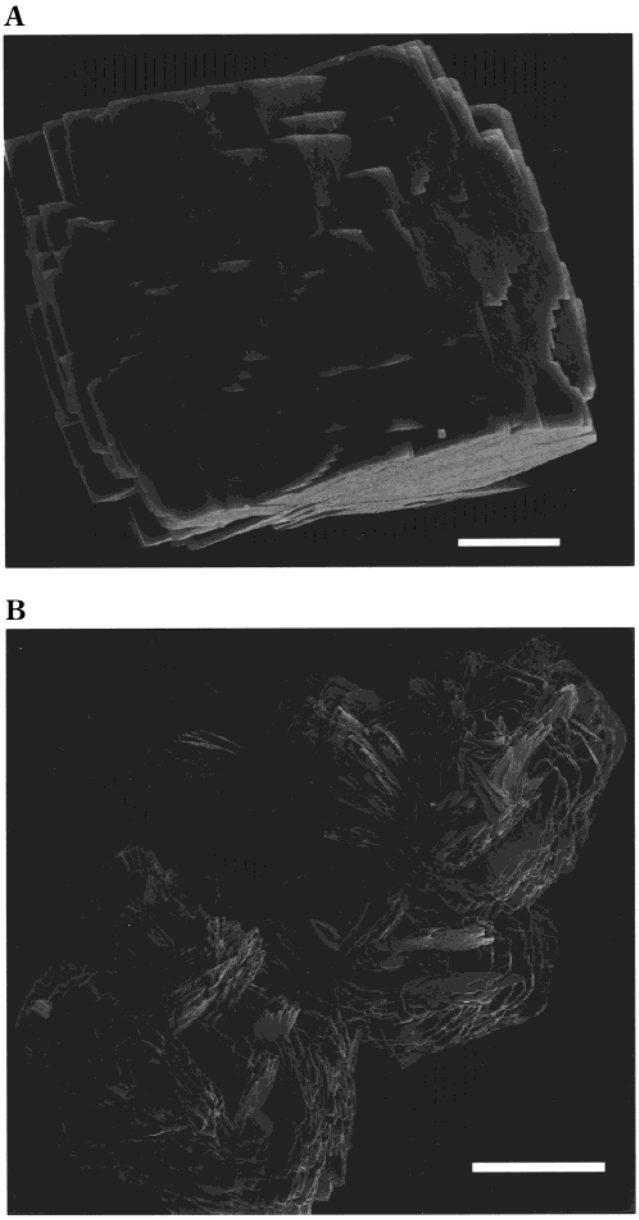

Figure 8. (A) Scanning electron microscopic image of $MnMoO_4 \cdot H_2O$ as prepared from $MnSO_4 \cdot H_2O$ and $Na_2MoO_4 \cdot 2H_2O$, illustrating prevalent twinning. Bar = 10 μm. (B) Scanning electron microscopic image of $MnMoO_4 \cdot H_2O$ as prepared from $MnSO_4 \cdot H_2O$ and $(NH_4)_2MoO_4$. Bar = 100 μm.

powder identified above as **3**. Apparently, the larger potassium cation provides stabilization of the complex oxide phase (**2**), perhaps through more efficient filling of the channels formed by the manganese and molybdate moieties in this structure (Figure 6). The corresponding sodium-containing phase, in contrast, is metastable, undergoing facile conversion to the more stable hydrated manganese molybdenum oxide phase (**3**) under ambient conditions.

Use of ammonium molybdate affords the same $MnMoO_4 \cdot H_2O$ phase (**3**) as obtained when using the sodium salt, albeit in reduced yield. Scanning electron microscopy again reveals the formation of complex crystalline intergrowths. Qualitative differences in morphology from the material obtained from sodium molybdate are evident (Figure 8B), with the ammonium salt affording intergrowths of platelike crystals, in contrast to the more three-dimensional crystals comprising the intergrowths obtained from the sodium salt (Figure 8A). Similar, but more pronounced countercation effects on crystal morphology are observed in the tungstate series (vide infra).

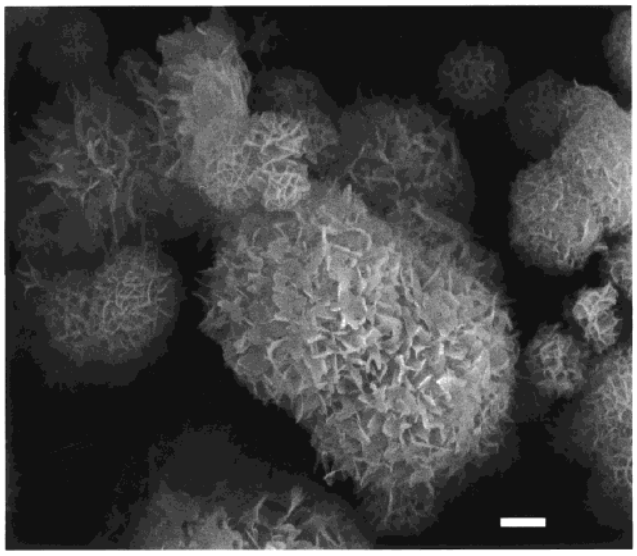

Figure 9. Scanning electron microscopic image of $MnWO_4 \cdot 0.8H_2O$. Bar = 1 μm.

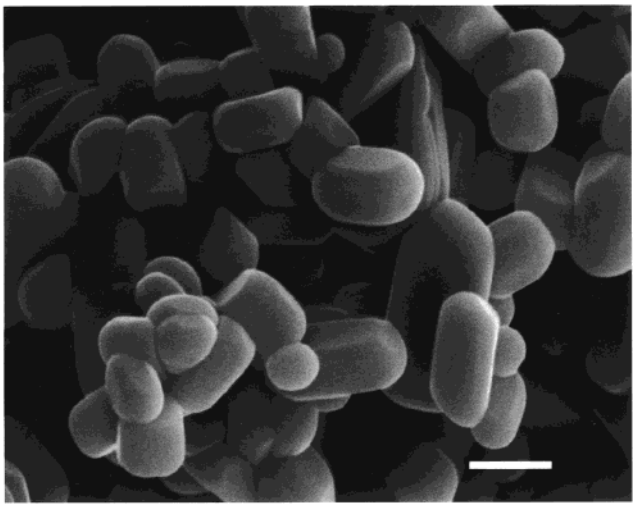

Figure 10. Scanning electron microscopic image of $MnWO_4 \cdot 0.8H_2O$ after TGA. Bar = 1 μm.

Earlier studies of related metathesis reactions led to the conclusion that the pH of the reaction mixture dictates which of three distinct $MnMoO_4 \cdot H_2O$ phases is obtained.[11] However, pH does not appear to be responsible for the cation-dependent phase selectivity of our metathesis reactions: the reaction mixtures from potassium, sodium, and ammonium molybdate all display very similar pH values (5.58, 5.22, and 5.12, respectively).

Tungstates. Salt metathesis reactions between manganese(II) salts (sulfate, chloride, and acetate) and Na_2WO_4 under conditions analogous to those used for the chromates and molybdates afford a hydrated manganese tungsten oxide, $MnWO_4 \cdot H_2O$ (**4**), as a pale-yellow solid. This compound is reproducibly obtained in the form of spherical microcrystalline aggregates (Figure 9). EDX analysis suggests the presence of only manganese and

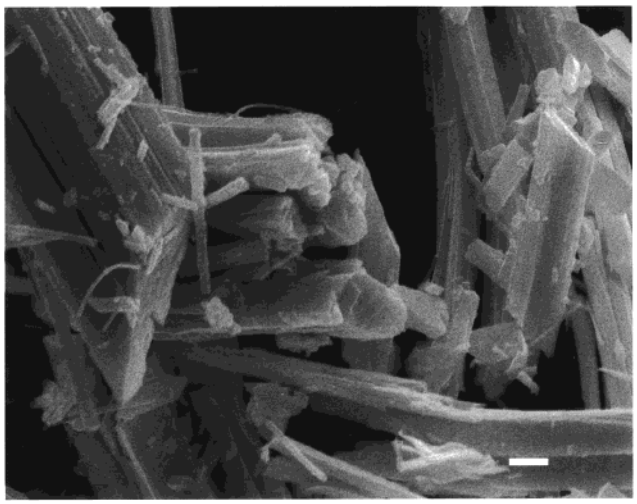

Figure 11. Scanning electron microscopic image of $MnWO_4 \cdot 0.8H_2O$ prepared from $(NH_4)_2WO_4$. Bar = 1 μm.

tungsten, with no evidence for incorporation of alkali metal cations. Differential scanning calorimetry (DSC) demonstrates a broad, irreversible exotherm at ca. 210 °C, and TGA confirms this feature is due to dehydration (Table 6). X-ray powder diffraction analysis after the DSC study demonstrates clean conversion to hübnerite, the only known anhydrous $MnWO_4$ phase, which is obtained in the form of somewhat rounded prisms (Figure 10). Interestingly, use of $(NH_4)_2WO_4$ in place of Na_2WO_4 in the salt metathesis reaction affords the same hydrated phase (**4**), but in more distinct single crystals than those obtained from the sodium salt (Figure 11). From both this result and that for the preparation of $MnMoO_4 \cdot H_2O$ (cf. Figure 8), it is apparent that the countercation can play a significant role in controlling crystal morphology of these oxide phases, presumably due to cation-selective interactions with various developing crystal surfaces.[26]

Summary

A series of manganese group 6 metal oxides may be readily prepared via salt metathesis reactions from aqueous solutions of manganese(II) salts and various chromate, molybdate, and tungstate salts. Regardless of the nature of the counterions, the chromate reactions invariably form a previously unknown phase, $KMn_2(CrO_4)_2(OH)(H_2O)$ (**1**), while the tungstate reactions afford a simpler, hydrated phase, $MnWO_4 \cdot H_2O$ (**4**). In these reactions, the countercation plays a significant role in determining crystal size and morphology. In contrast, molybdate reactions display a marked countercation-dependent phase selectivity. Sodium and ammonium molybdate afford hydrated manganese molybdenum oxide, $MnMoO_4 \cdot H_2O$ (**3**), whereas potassium molybdate affords the previously unknown molydenum analogue of the chromate phase, $KMn_2(MoO_4)_2(OH)(H_2O)$ (**2**). Counteranion effects are more subtle, with crystal form and size representing the primary differences between the products from reactions using sulfate, acetate, or chloride salts of manganese(II). Each phase undergoes thermal dehydration, affording α-$MnMoO_4$ from **3** and $MnWO_4$ (hübnerite) from **4**. Attempts to exploit solvent or chelation effects for the modification of crystal form in general reduced the crystallinity of the various oxide phases.

Acknowledgment. The support of this work by the Office of Naval Research is gratefully acknowledged.

Supporting Information Available: Details of crystallographic data collection and structure refinement for **2**. This material is available free of charge via the Internet at http://pubs.acs.org.

CM000754C

(26) In contrast to the molybdate series, pH may be playing a role in the crystal shape selectivity of these reactions: the ammonium tungstate reaction mixture is appreciably more acidic (pH 4.45) than the sodium tungstate (pH 8.17) and potassium tungstate (pH 8.52) reaction mixtures.